Supporting Information

Sass et al. 10.1073/pnas.1110385108

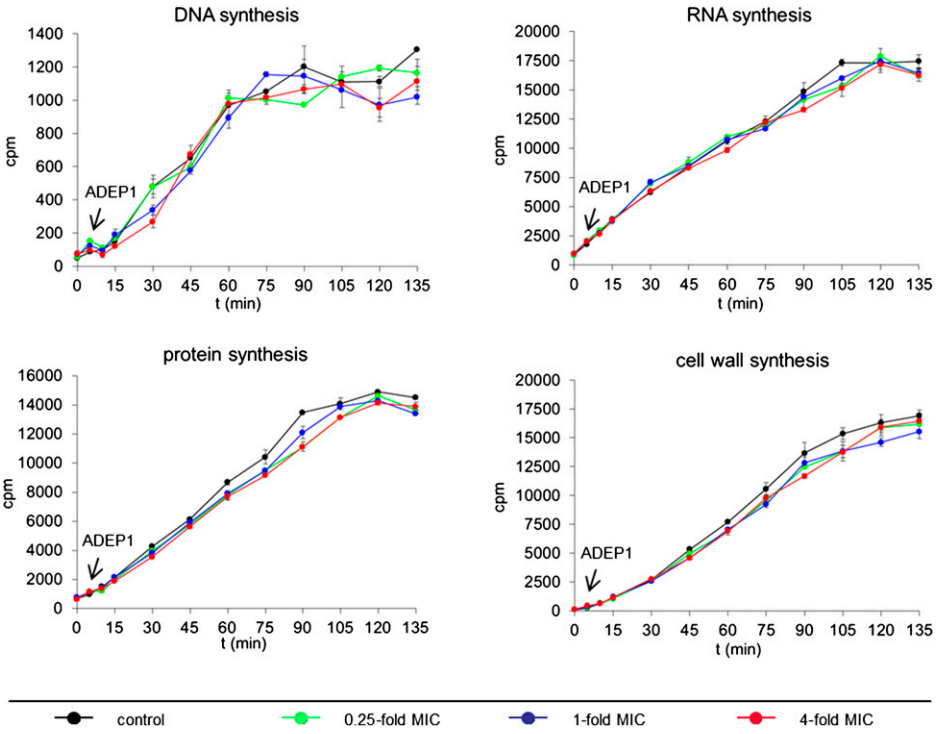

Fig. S1. Effects of ADEP on the synthesis of biopolymers by *B. subtilis* 168 determined by incorporation of radioactive precursors. *B. subtilis* was grown in defined minimal broth Davis without dextrose (Difco) supplemented with 0.025% Bacto-Pepton and 5 mL/L glycerol (87%), and the incorporation of [^{14}C]-thymidine (DNA synthesis), [^{14}C]-uridine (RNA synthesis), [^{14}C]-leucine (protein synthesis), and [^{14}C]-glucosamine (cell wall synthesis) into acid-precipitable macromolecules of *B. subtilis* 168 was measured as described previously (1). Cultures were incubated with ADEP1 at concentrations of 0.05, 0.2, or 0.78 μg/mL, corresponding to 0.25, one, or four times the MIC, respectively. Even at four times the MIC, ADEP1 did not inhibit any of the tested biosynthetic pathways. Instead, cells continued to produce biomass and formed filaments (compare Fig. 1). Incorporation assays were performed in duplicate and error bars represent absolute deviations from the respective mean value.

1. Freiberg C, et al. (2004) Identification and characterization of the first class of potent bacterial acetyl-CoA carboxylase inhibitors with antibacterial activity. *J Biol Chem* 279: 26066–26073.

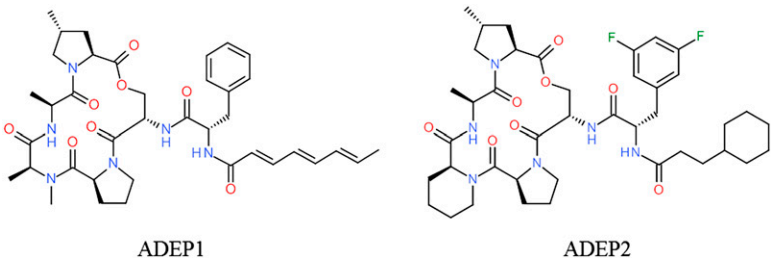

Fig. S2. Structure of ADEP1 and its synthetic congener ADEP2. The natural product ADEP1 and its optimized synthetic congener ADEP2 demonstrate MICs in the submicrogram/milliliter range against staphylococci, streptococci, and enterococci, and their efficacy in rodent models of bacterial infection surpassed the activity of the marketed Gram-positive problem solver antibiotic linezolid (1).

1. Brötz-Oesterhelt H, et al. (2005) Dysregulation of bacterial proteolytic machinery by a new class of antibiotics. *Nat Med* 11:1082–1087.

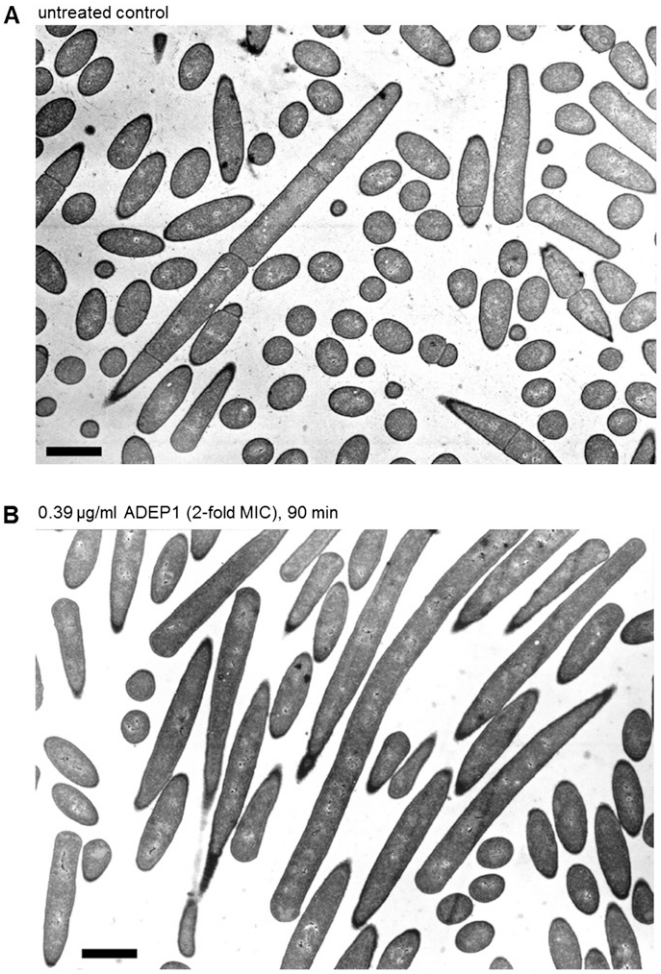

Fig. S3. Electron micrographs of *B. subtilis* 168 in the absence or presence of ADEP. For EM, *B. subtilis* cells were grown at 37 °C in Iso-Sensitest broth to an OD_{600} of 0.1. Then, cells were treated with 0.39 µg/mL of ADEP1 (twice the MIC) and samples were taken after 90 min. Samples of treated cells and controls were further processed as described previously (1). Images were acquired using a Philips EM400 electron microscope. (*A*) Untreated control cells. In cases, where the section plane parallels the long axis of the cells, complete and regular septa are detected. (*B*) Cells that have been treated with ADEP1 are completely devoid of septa. Not even regions of septum initiation are left. (Scale bars, 2 µm.)

1. Pauluhn J, Emura M, Mohr U, Popp A, Rosenbruch M (1999) Two-week inhalation toxicity of polymeric diphenylmethane-4, 4′-diisocyanate (PMDI) in rats: Analysis of biochemical and morphological markers of early pulmonary response. *Inhal Toxicol* 11:1143–1163.

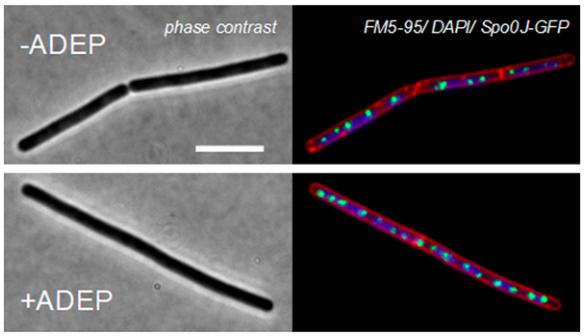

Fig. S4. Localization of Spo0J–GFP during ADEP treatment. The fluorescence images show overlays of FM5-95 (red, membrane), DAPI (blue, nucleoid), and GFP (green, Spo0J) channels. Localization of GFP-tagged Spo0J in *B. subtilis* 168 strain HM160 was visualized after 60 min in the absence or presence of 0.25 µg/mL ADEP2. Nucleoid segregation and localization of Spo0J remained unperturbed in the presence of ADEP, implying that deficiencies in nucleoid segregation can be excluded for the inhibition of Z-ring assembly. (Scale bars, 5 µm.)

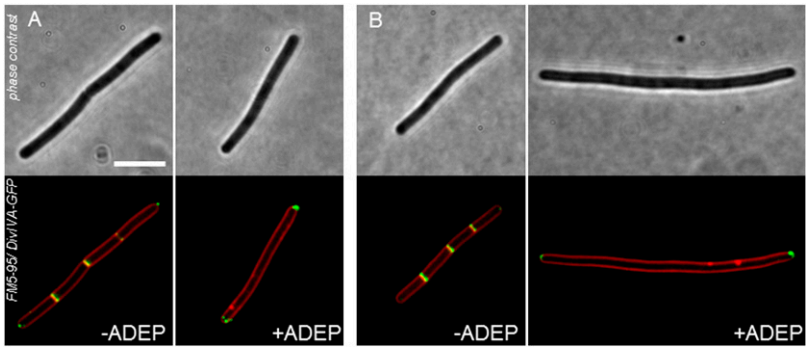

Fig. S5. Localization of DivIVA–GFP during ADEP treatment. The fluorescence images show overlays of GFP (green, DivIVA) and FM5-95 (red, membrane) channels. Localization of GFP-tagged DivIVA in *B. subtilis* 168 strain 1803 was visualized after (*A*) 30 min and (*B*) 60 min in the absence or presence of 0.25 μg/mL ADEP2. Here, DivIVA still targets the cell poles of ADEP-treated cells; however, it is no longer recruited to the prospective cell division sites. (Scale bars, 5 μm.)

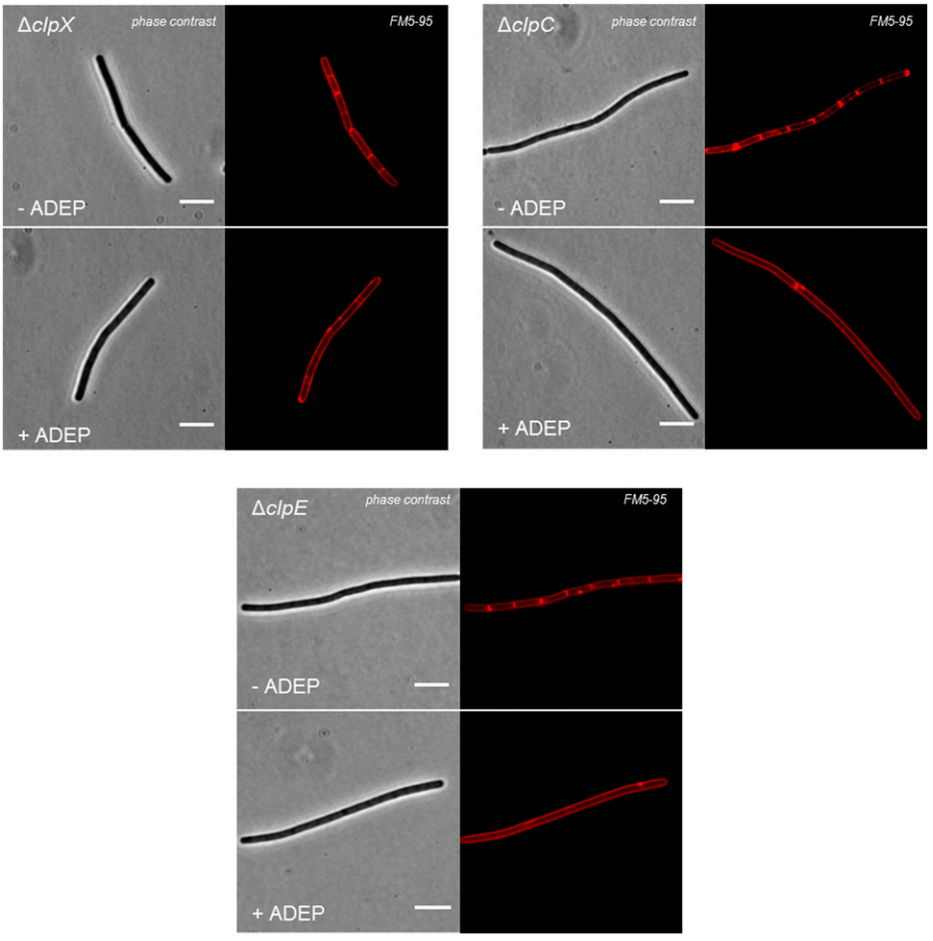

Fig. S6. Impact of *clpX*, *clpC*, and *clpE* deletions on the inhibition of septum formation. Septum formation in Clp ATPase deletion mutants was visualized using FM5-95 membrane dye. Here, the *clpX*, *clpC*, and *clpE* single deletions did not suppress the inhibition of septum formation by ADEP, showing that ADEP-induced inhibition of Z-ring assembly does not require the presence of Clp ATPases. (Scale bars, 5 μm.) Strains used: *B. subtilis* BEK90 (Δ*clpX*), *B. subtilis* QPB418 (Δ*clpC*), and *B. subtilis* BMM03 (Δ*clpE*).

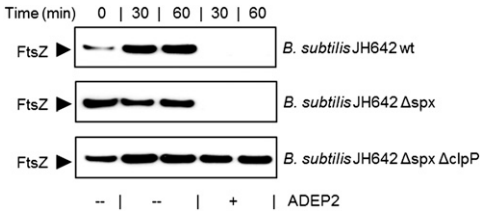

Fig. S7. ClpP-dependent degradation of FtsZ in bacterial cells. Immunodetection of FtsZ was performed using anti-FtsZ antibodies. ADEP treatment of exponentially growing wild-type cells of *B. subtilis* JH642 and the control strain *B. subtilis* JH642 Δ*spx* resulted in a complete loss of the FtsZ signal after 30 min. However, no decrease of the FtsZ signal was observed in the clpP deletion background of strain *B. subtilis* JH642 Δ*spx* Δ*clpP*, indicating the essential role of ClpP for ADEP activity.

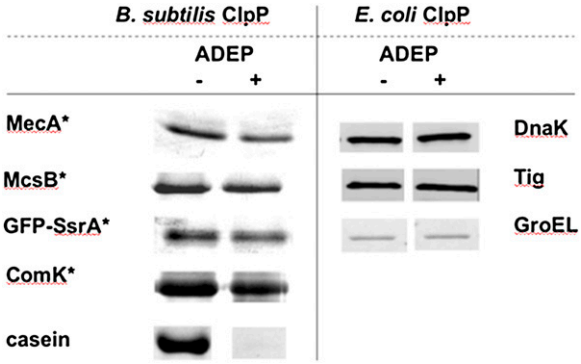

Fig. S8. The ADEP-activated isolated ClpP prefers flexible proteins to folded proteins with defined structures. Attempts to degrade various folded, stable proteins by the ADEP-dysregulated ClpP cores of either *B. subtilis* or *E. coli* failed. In contrast, the flexible casein was rapidly degraded. Asterisks mark substrates of the Clp protease, which are known to be degraded by ClpP/Clp-ATPase complexes in the physiological context. These degradation assays were performed here with purified ClpP ± ADEP in the absence of Clp ATPases.

Table S1. Bacterial strains and plasmids

	Relevant characteristic(s) or genotype	Used induction	Reference or source
Strains			
B. subtilis			
168	*trpC2*; WT strain	—	1
2020	*trpC2 spc amyE::Pxyl-gfp-ftsZ*	0.1% xylose	2
1803	*trpC2 cat divIVA-gfp*	—	3
HM160	*trpC2 neo spo0J-gfp*	—	4
QB4916	*trpC2 ΔclpP::spc*	—	5
BEK90	*trpC2 ΔclpX::kan* in *B. subtilis* 168 background	—	6
QPB418	*trpC2 ΔclpC::tet*	—	7
BMM03	*trpC2 ΔclpE::spc*	—	8
PY79	prototrophic derivative of *B. subtilis* 168	—	9
BJK424	PY79; *spx::erm*	—	10
BJK474	PY79; *spx::erm clpP-gfp spc clpE::tet clpC::cat clpX::kan*	—	10
JH642	*trpC2 pheA1*	—	11
ORB3834	*trpC2 pheA1 spx::neo*	—	11
ORB3839	*trpC2 pheA1 spx::neo clpP::erm*	—	11
S. aureus			
HG001	NCTC8325 derivative, *rsbU* repaired, *tcaR*	—	12
RNpPBP2-31	RN4220 derivative with *gfp-pbp2* fusion	0.1% xylose	13
S. pneumoniae			
G9A	Clinical isolate from human infections		14
E. coli			
K-12 JM109	Subcloning host	—	15
Bl21(DE3)	λDE3 lysogen; expression host	—	16
W3110 (pBS58)(pCXZ)	Strain W3110 carrying the plasmids pCXZ(Ptac-*ftsZ*bs, Amp^R) and pBS58 (*ftsQAZ*ec, Spc^R)	0.5 mM IPTG	17
Plasmids			
pClpP11	pQE70 + ORF BSU34540 (*clpP*) of *B. subtilis* 168	0.5 mM IPTG	18

1. Anagnostopoulos C, Spizizen J (1961) Requirements for transformation of *Bacillus subtilis*. *J Bacteriol* 81:741–746.
2. Stokes NR, et al. (2005) Novel inhibitors of bacterial cytokinesis identified by a cell-based antibiotic screening assay. *J Biol Chem* 280:39709–39715.
3. Edwards DH, Thomaides HB, Errington J (2000) Promiscuous targeting of *Bacillus subtilis* cell division protein DivIVA to division sites in *Escherichia coli* and fission yeast. *EMBO J* 19: 2719–2727.
4. Strahl H, Hamoen LW (2010) Membrane potential is important for bacterial cell division. *Proc Natl Acad Sci USA* 107:12281–12286.
5. Msadek T, et al. (1998) ClpP of *Bacillus subtilis* is required for competence development, motility, degradative enzyme synthesis, growth at high temperature and sporulation. *Mol Microbiol* 27:899–914.
6. Gerth U, et al. (2004) Fine-tuning in regulation of Clp protein content in *Bacillus subtilis*. *J Bacteriol* 186:179–191.
7. Pan Q, Garsin DA, Losick R (2001) Self-reinforcing activation of a cell-specific transcription factor by proteolysis of an anti-sigma factor in *B. subtilis*. *Mol Cell* 8:873–883.
8. Miethke M, Hecker M, Gerth U (2006) Involvement of *Bacillus subtilis* ClpE in CtsR degradation and protein quality control. *J Bacteriol* 188:4610–4619.
9. Youngman P, Perkins JB, Losick R (1984) Construction of a cloning site near one end of Tn917 into which foreign DNA may be inserted without affecting transposition in *Bacillus subtilis* or expression of the transposon-borne *erm* gene. *Plasmid* 12:1–9.
10. Kain J, He GG, Losick R (2008) Polar localization and compartmentalization of ClpP proteases during growth and sporulation in *Bacillus subtilis*. *J Bacteriol* 190:6749–6757.
11. Nakano MM, Hajarizadeh F, Zhu Y, Zuber P (2001) Loss-of-function mutations in *yjbD* result in ClpX- and ClpP-independent competence development of *Bacillus subtilis*. *Mol Microbiol* 42:383–394.
12. Herbert S, et al. (2010) Repair of global regulators in *Staphylococcus aureus* 8325 and comparative analysis with other clinical isolates. *Infect Immun* 78:2877–2889.
13. Pinho MG, Errington J (2003) Dispersed mode of *Staphylococcus aureus* cell wall synthesis in the absence of the division machinery. *Mol Microbiol* 50:871–881.
14. Beyer D, et al. (2004) New class of bacterial phenylalanyl-tRNA synthetase inhibitors with high potency and broad-spectrum activity. *Antimicrob Agents Chemother* 48:525–532.
15. Yanisch-Perron C, Vieira J, Messing J (1985) Improved M13 phage cloning vectors and host strains: Nucleotide sequences of the M13mp18 and pUC19 vectors. *Gene* 33:103–119.
16. Studier FW, Moffatt BA (1986) Use of bacteriophage T7 RNA polymerase to direct selective high-level expression of cloned genes. *J Mol Biol* 189:113–130.
17. Wang X, Lutkenhaus J (1993) The FtsZ protein of *Bacillus subtilis* is localized at the division site and has GTPase activity that is dependent upon FtsZ concentration. *Mol Microbiol* 9: 435–442.
18. Turgay K, Hahn J, Burghoorn J, Dubnau D (1998) Competence in *Bacillus subtilis* is controlled by regulated proteolysis of a transcription factor. *EMBO J* 17:6730–6738.